Infection and Immunity

Molecular Characterization of UpaB and UpaC, Two New Autotransporter Proteins of Uropathogenic Escherichia coli CFT073

Luke P. Allsopp, Christophe Beloin, Glen C. Ulett, Jaione Valle, Makrina Totsika, Orla Sherlock, Jean-Marc Ghigo and Mark A. Schembri

Infect. Immun. **2012, 80(1):321. DOI: 10.1128/IAI.05322-11. Published Ahead of Print 19 September 2011.**

Updated information and services can be found at:
http://iai.asm.org/content/80/1/321

These include:

REFERENCES This article cites 81 articles, 47 of which can be accessed free at: http://iai.asm.org/content/80/1/321#ref-list-1

CONTENT ALERTS Receive: RSS Feeds, eTOCs, free email alerts (when new articles cite this article), more»

Information about commercial reprint orders: **http://iai.asm.org/site/misc/reprints.xhtml**
To subscribe to to another ASM Journal go to: **http://journals.asm.org/site/subscriptions/**

Journals.ASM.org

Downloaded from http://iai.asm.org/ on December 23, 2011 by INSTITUT PASTEUR-Médiathèque

IAI
Journals.ASM.org

Molecular Characterization of UpaB and UpaC, Two New Autotransporter Proteins of Uropathogenic *Escherichia coli* CFT073

Luke P. Allsopp,[a] Christophe Beloin,[b,c] Glen C. Ulett,[d] Jaione Valle,[b,c]* Makrina Totsika,[a] Orla Sherlock,[a]* Jean-Marc Ghigo,[b,c] and Mark A. Schembri[a]

Australian Infectious Disease Research Centre, School of Chemistry and Molecular Biosciences, University of Queensland, Brisbane, QLD, Australia,[a] Institut Pasteur, Unité de Génétique des Biofilms, Département de Microbiologie, Paris, France,[b] CNRS, URA2172, Paris, France,[c] and Centre for Medicine and Oral Health Campus, Griffith University, Southport, QLD, Australia[d]

Uropathogenic *Escherichia coli* (UPEC) is the primary cause of urinary tract infection (UTI) in the developed world. The major factors associated with virulence of UPEC are fimbrial adhesins, which mediate specific attachment to host receptors and trigger innate host responses. Another group of adhesins is represented by the autotransporter (AT) subgroup of proteins. The genome-sequenced prototype UPEC strain CFT073 contains 11 putative AT-encoding genes. In this study, we have performed a detailed molecular characterization of two closely related AT adhesins from CFT073: UpaB (c0426) and UpaC (c0478). PCR screening revealed that the *upaB* and *upaC* AT-encoding genes are common in *E. coli*. The *upaB* and *upaC* genes were cloned and characterized in a recombinant *E. coli* K-12 strain background. This revealed that they encode proteins located at the cell surface but possess different functional properties: UpaB mediates adherence to several ECM proteins, while UpaC expression is associated with increased biofilm formation. In CFT073, *upaB* is expressed while *upaC* is transcriptionally repressed by the global regulator H-NS. In competitive colonization experiments employing the mouse UTI model, CFT073 significantly outcompeted its *upaB* (but not *upaC*) isogenic mutant strain in the bladder. This attenuated phenotype was also observed in single-challenge experiments, where deletion of the *upaB* gene in CFT073 significantly reduced early colonization of the bladder.

Urinary tract infections (UTIs) are among the most frequent human bacterial infections, with an estimated 40 to 50% of women experiencing at least one cystitis episode in their lifetime (19, 34). UTI usually starts as a bladder infection (cystitis) but can develop to acute kidney infection (pyelonephritis), ultimately resulting in scaring and renal failure. UTI is also a major cause of sepsis, which has a mortality rate of 25% and results in more than 36,000 deaths per year in the United States (66). Almost all patients with an indwelling urinary catheter for 30 days or longer develop catheter-associated UTI, which accounts for approximately 40% of all hospital-acquired infections (19).

Uropathogenic *Escherichia coli* (UPEC) is the most common etiological agent responsible for UTI, resulting in more than 80% of infections. UPEC strains possess an array of virulence factors, with no factor solely responsible for the ability to cause UTI (49). However, the ability of UPEC to colonize the urinary tract and cause disease involves the expression of adhesins (e.g., type 1 and P fimbriae), toxins (e.g., hemolysin), and iron acquisition systems that utilize siderophores (e.g., enterobactin, salmochelin, aerobactin) (36, 78). Adherence to the urinary tract epithelium enables bacteria to resist the hydrodynamic forces of urine flow, to trigger host and bacterial cell signaling pathways, and to establish infection. Among adhesins, P and type 1 fimbriae correlate strongly with uropathogenesis and mediate binding to specific receptors within the urinary tract (11, 46, 53, 67, 79, 80). Both P and type 1 fimbriae recognize their receptor targets by virtue of organelle tip-located adhesins, PapG and FimH, respectively (31, 38). Recent work employing a rat infection model has also demonstrated that P and type 1 fimbriae can act in synergy to establish an infection that leads to nephron obstruction within the kidneys (42).

In addition to fimbrial adhesins, a number of autotransporter (AT) proteins associated with virulence have been characterized from UPEC. These include the secreted toxin Sat (21, 22), the phase variable outer membrane protein antigen 43 (Ag43) (69), the trimeric AT protein UpaG (72), and the surface-located UpaH (1). AT proteins represent the largest group of bacterial type V secreted proteins and share several common features: an N-terminal signal sequence, a passenger (α) domain that is either anchored to the cell surface or released into the external milieu, and a translocation (β) domain that resides in the outer membrane (27, 32). AT proteins were originally thought to possess structural properties that facilitate their independent transport across the bacterial membrane system and final routing to the cell surface (28). However, this classical view has recently been called into question, as accessory factors, such as the Bam complex (also known as the YaeT or Omp85 complex), as well as periplasmic chaperones, such as SurA, Skp, and DegP, are required for the secretion of some AT proteins (30, 51, 56, 57, 59, 74). In general, AT proteins differ substantially in their passenger domain sequence, which determines the unique functional characteristics of the protein and is often associated with virulence (28).

Received 5 May 2011 Returned for modification 6 June 2011
Accepted 7 September 2011
Published ahead of print 19 September 2011
Editor: J. B. Bliska

Address correspondence to Mark A. Schembri, m.schembri@uq.edu.au.
* Present address: J. Valle, Laboratory of Microbial Biofilms, Instituto de Agrobiotecnologia, Universidad Pública de Navarra-CSIC-Gobierno de Navarra, Pamplona, Spain; O. Sherlock, Department of Applied Sciences, Dundalk Institute of Technology, Dundalk, Ireland.

Copyright © 2012, American Society for Microbiology. All Rights Reserved.

doi:10.1128/IAI.05322-11

Downloaded from http://iai.asm.org/ on December 23, 2011 by INSTITUT PASTEUR-Médiathèque

Eleven putative AT-encoding genes have been identified in the sequenced genome of the prototype UPEC strain CFT073 (1, 50). The biological significance of these AT proteins and their roles in UPEC pathogenesis remain to be fully elucidated. In this study, we have performed a detailed molecular characterization of two of these AIDA-I-type conventional AT proteins, namely, UpaB (c0426) and UpaC (c0478). The *upaB* and *upaC* genes were cloned, and expression of UpaC significantly increased biofilm formation in a recombinant strain. Using Western blot analysis, we showed that UpaB (but not UpaC) is expressed by CFT073. UpaC was shown to be transcriptionally repressed by the global regulator H-NS, and mutation of the *hns* gene relieved this repression. In the mouse UTI model, deletion of *upaB* (but not *upaC*) in CFT073 significantly reduced early colonization of the bladder.

MATERIALS AND METHODS

Bacterial strains and growth conditions. The strains and plasmids used in this study are listed in Table 1. Cells were routinely grown at 28°C or 37°C on solid or in liquid lysogeny broth (LB) medium (7) supplemented with the appropriate antibiotics, kanamycin (Kan; 50 μg/ml), chloramphenicol (Cam; 25 μg/ml), ampicillin (Amp; 100 μg/ml), spectinomycin (Spec; 50 μg/ml), and zeocin (Zeo; 50 μg/ml). For growth in defined conditions, M9 and M63B1 glucose media (58) were used as indicated. Bacterial cultures for mouse experiments were prepared by overnight growth in LB broth; all strains displayed an equivalent level of type 1 fimbriae expression as assessed by yeast cell agglutination.

DNA manipulations and genetic techniques. DNA techniques were performed as described by Sambrook and Russell (58). Isolation of plasmid DNA was carried out using the QIAprep spin miniprep kit (Qiagen). Restriction endonucleases were used according to the manufacturer's specifications (New England BioLabs). Chromosomal DNA purification was made using the DNeasy blood and tissue kit (Qiagen). Oligonucleotides were purchased from Sigma, Australia, or France. All PCRs requiring proofreading were performed with the Expand high-fidelity polymerase system (Roche) as described by the manufacturer. Amplified products were sequenced to ensure fidelity of the PCR. DNA sequencing was performed using the ABI BigDye version 3.1 kit (ABI) by the Australian Equine Genetics Research Centre, University of Queensland, Brisbane. Prevalence studies for the *upaB* and *upaC* genes used *Taq* DNA polymerase, as described by the manufacturer (New England BioLabs), with the primers c0426.s-5 (5′-GGAAAGGCAAAGTTTCAGGG) and c0426.s-3 (5′-GGTGGTATGTTTCTGTTTAC) or c0478.s-5 (5′-GGTGGTTGGGTAGATGC) and c0478.s-3 (5′-GTTCACATCCAGTACACCAC).

Construction of plasmids with AT-encoding genes. The *upaB* and *upaC* genes were amplified by PCR from UPEC CFT073 using specific primers designed from the available genome sequence. The following primers were used: for *upaB* (c0426), P1 (5′-CGCGCTCGAGATAATAAGGAATGGGAAATTGAAATTAGTTAC) and P2 (5′-CGGCGAAGCTTTTACCAGGTCACATTGATAC); and for *upaC* (c0478), P3 (5′-CGCGCTCGAGATAATAAGGATGACAAATGCACTCCTG) and P4 (5′-CGGCGGAATTCTTACCAGGTATATTTAACAC). PCR products containing *upaB* and *upaC* were digested with XhoI (forward primer) and HindIII/EcoRI (reverse primer) and ligated to XhoI-HindIII/EcoRI-digested plasmid pBAD/*Myc*-HisA. The resultant plasmids were then digested with HindIII (*upaB* plasmid) or EcoRI (*upaC* plasmid) and ligated with a correspondingly digested kanamycin resistance-encoding gene cassette to give rise to plasmids pUpaB (pOMS14) and pUpaC (pOMS12). Resistance to kanamycin was required to facilitate transformation of these plasmids into the *flu*-negative, *gfp*-positive *E. coli* K-12 strain OS56. In all constructs, expression of the AT-encoding gene is under the control of the arabinose-inducible *araBAD* promoter (23). Neither of the genes was cloned as fusions to the 6×His-encoding sequence of the expression plasmid. Plasmids were verified by sequence analysis. The *hns* gene (c1701) was subcloned from pBAD30*c1701* (37) via digestion with NheI/SphI and ligated to NheI/SphI-digested pBR322, creating pH-NS.

Construction of deletion and overexpression mutants. In order to interrupt the AT-encoding genes in CFT073, create *lacZ* reporter transcriptional fusions, and place chromosomal target genes under the control of the RExBAD promoter or PcL promoter (13, 14, 55), we used homologous recombination mediated by λ-red recombinase expressed from the pKOBEG plasmid (15) and either a one-step PCR procedure with 40-bp homology arms for recombination or a three-step PCR procedure with 500-bp homology arms for recombination (15) (http://www.pasteur.fr/recherche/unites/Ggb/matmet.html). All mutants were confirmed via PCR and sequencing using primers Gene.ext 5′ and Gene.ext 3′, either as a primer set or individually in combination with internal primers designed to bind within the inserted DNA fragments. The full list of primers is available at http://www.pasteur.fr/recherche/unites/Ggb/submat.html. CFT073*lacI-Z upaC*::*lacZ-zeo* mutants were screened after mutagenesis with the suicide plasmid pSC189, carrying the kanamycin-resistant Mariner transposon described previously (10, 12). Sequencing out from the transposon in both directions enabled the site of insertion to be identified.

Purification of 6×His-tagged UpaB and UpaC truncated proteins, antibody production, and immunoblotting. A 1,219-bp segment from the passenger-encoding domain of *upaB* was amplified by PCR with primers UpaBTF (5′-TACTTCCAATCCAATGCCACGGTATCAACTGATCCGG) and UpaBTR (5′-TTATGCACTTCCAATGTTATGTGGCTTTTAGAGTGCTGTC) from *E. coli* CFT073 genomic DNA (underlined nucleotides represent the ligation-independent cloning [LIC] overhangs used for insertion into plasmid pMCSG7 via LIC cloning) (16). The resultant plasmid (pUpaBTruncated) contained the base pairs 102 to 1,320 of *upaB* fused to a 6×His-encoding sequence. *E. coli* BL21 was transformed with plasmid pUpaBTruncated and induced with IPTG (isopropyl-β-D-thiogalactopyranoside), and the resultant 6×His-tagged UpaB truncated protein (containing amino acids 35 to 440 of UpaB) was assessed by SDS-PAGE analysis as previously described (70). Polyclonal anti-UpaB serum was raised in rabbits by the Institute of Medical and Veterinary Sciences (South Australia). A polyclonal antibody raised against the enterohemorrhagic *E. coli* homologue of UpaC, EhaB, cross-reacted with UpaC and was used for UpaC detection (75). It is referred in this report as anti-UpaC antiserum. For immunoblotting, whole-cell lysates were subjected to SDS-PAGE using NuPAGE Novex 4 to 12% Bis-Tris precast gels with NuPAGE MES (morpholineethanesulfonic acid) running buffer and subsequently transferred to polyvinylidene difluoride (PVDF) microporous membrane filters using the iBlot dry-blotting system as described by the manufacturer (Invitrogen). UpaB or UpaC antiserum, respectively, was used as the primary serum, and the secondary antibody was alkaline phosphatase-conjugated anti-rabbit IgG. Sigma Fast BCIP/NBT was used as the substrate in the detection process.

Biofilm assays. Biofilm formation on polystyrene surfaces was monitored by using 96-well microtiter plates (IWAKI) essentially as previously described (63). Briefly, cells were grown for 24 h in LB (containing 0.2% arabinose for induction of AT-encoding genes) at 37°C, washed to remove unbound cells, and stained with crystal violet. Quantification of bound cells was performed by the addition of acetone-ethanol (20:80) and the measurement of the dissolved crystal violet at an optical density of 570 nm (OD_{570}). Flow chamber experiments were performed as previously described (35, 62). Briefly, biofilms were allowed to form on glass surfaces in a multichannel flow system that permitted online monitoring of their structural characteristics. Flow cells were inoculated with standardized cultures (OD_{600} = 0.02) pregrown overnight in M9 medium containing arabinose and kanamycin. Biofilm development was monitored by confocal scanning laser microscopy at 15 h postinoculation. For analysis of flow cell biofilms, z-stacks were analyzed using COMSTAT software program (29). Microfermentor experiments were performed as previously described (5, 20). Briefly, overnight cultures were grown in M63B1-0.4% glucose medium in the presence and absence of 0.2% arabinose at 37°C. Inoculation was performed by dipping the removable spatula in a culture

Downloaded from http://iai.asm.org/ on December 23, 2011 by INSTITUT PASTEUR-Médiathèque

TABLE 1 Bacterial strains and plasmids used in this study

Strain or plasmid	Relevant characteristic(s)	Reference
E. coli K12 strains		
MS427	MG1655*flu*	52
OS56	MG1655*flu attB::bla-gfp* GFP$^+$, Amp^r	64
MS427(pBAD)	MS427 pBADMycHisA, Amp^r	76
MS427(pUpaC)	pUpaC in MS427, Amp^r	This study
MS427(pUpaB)	pUpaB in MS427, Amp^r	This study
OS56(pBAD)	OS56 pBADMycHisA	76
OS56(pUpaC)	pUpaC in OS56, Amp^r Kan^r	This study
OS56(pUpaB)	pUpaB in OS56, Amp^r Kan^r	This study
BL21	F$^-$ *ompT hsdS*(r_B^- m_B^-) *dcm gal*	Stratagene
MS2930	BL21 pUpaBTruncated	This study
S17-1λpir	RP4-2Tc::mu *kan*::Tn*7* λpir; Pir-dependent replication, Mu^r Kan^r	65
S17-1λpir_pSC189	pSC189 in S17-1λpir, Amp^r Kan^r	12
E. coli CFT073 strains		
CFT073	Wild-type UPEC isolate	44
CFT073*ara*	CFT073 *araDAB*::*zeo*, Zeo^r	This study
CFT073^{amp}	CFT073 *attB*::*amp-cfp*, Amp^r	18
RExUpaB	CFT073*ara cam*RExBAD*upaB*, Zeo^r Cam^r, arabinose inducible UpaB	This study
RExUpaC	CFT073*ara spec*RExBAD*upaC*, Zeo^r Spec^r, arabinose inducible UpaC	This study
CFT073*upaB*	CFT073*upaB*::*zeo*, Zeo^r	This study
CFT073*upaC*	CFT073*upaC*::*kan*, Kan^r	This study
CFT073PcL*upaB*	CFT073 *kan*PcL*upaB*, constitutively expressed UpaB, Kan^r	This study
CFT073PcL*upaC*	CFT073 *kan*PcL*upaC*, constitutively expressed UpaC, Kan^r	This study
CFT073*lacIZ*	CFT073*lacIZ*::*cam*, Cam^r	This study
CFT073*lacIZ upaB*::*lacZ-zeo*	CFT073*lacIZ*::*cam upaB*::*lacZ-zeo*, Cam^r Zeo^r	This study
CFT073*lacIZ upaB*::*lacZ-zeo c1701*::*kan*	CFT073*lacIZ*::*cam upaB*::*lacZ-zeo c1701*::*kan*, Cam^r Zeo^r Kan^r	This study
CFT073*lacIZ upaB*::*lacZ-zeo c1701*::*kan* pBR322	CFT073*lacIZ*::*cam upaB*::*lacZ-zeo c1701*::*kan* pBR322, Cam^r Zeo^r Kan^r Amp^r	This study
CFT073*lacIZ upaB*::*lacZ-zeo c1701*::*kan* pH-NS	CFT073*lacIZ*::*cam upaB*::*lacZ-zeo c1701*::*kan* pH-NS, Cam^r Zeo^r Kan^r Amp^r	This study
CFT073*lacIZ upaC*::*lacZ-zeo*	CFT073*lacIZ*::*cam upaC*::*lacZ-zeo*, Cam^r Zeo^r	This study
CFT073*lacIZ upaC*::*lacZ-zeo c1701*::*kan*	CFT073*lacIZ*::*cam upaC*::*lacZ-zeo c1701*::*kan*, Cam^r Zeo^r Kan^r	This study
CFT073*lacIZ upaC*::*lacZ-zeo c1701*::*kan* pBR322	CFT073*lacIZ*::*cam upaC*::*lacZ-zeo c1701*::*kan* pBR322, Cam^r Zeo^r Kan^r Amp^r	This study
CFT073*lacIZ upaC*::*lacZ-zeo c1701*::*kan* pH-NS	CFT073*lacIZ*::*cam upaC*::*lacZ-zeo c1701*::*kan* p-NS, Cam^r Zeo^r Kan^r Amp^r	This study
CFT073*lacIZ upaB*::*lacZ-zeo c0421*::*kan*	CFT073*lacIZ*::*cam upaB*::*lacZ-zeo c0421*::*kan*, Cam^r Zeo^r Kan^r	This study
CFT073*lacIZ upaC*::*lacZ-zeo c0421*::*kan*	CFT073*lacIZ*::*cam upaC*::*lacZ-zeo c0421*::*kan*, Cam^r Zeo^r Kan^r	This study
CFT073*lacIZ upaB*::*lacZ-zeo c1699*::*kan*	CFT073*lacIZ*::*cam upaB*::*lacZ-zeo c1699*::*kan*, Cam^r Zeo^r Kan^r	This study
CFT073*lacIZ upaC*::*lacZ-zeo c1699*::*kan*	CFT073*lacIZ*::*cam upaC*::*lacZ-zeo c1699*::*kan*, Cam^r Zeo^r Kan^r	This study
CFT073*lacIZ upaB*::*lacZ-zeo c2091*::*kan*	CFT073*lacIZ*::*cam upaB*::*lacZ-zeo c2091*::*kan*, Cam^r Zeo^r Kan^r	This study
CFT073*lacIZ upaC*::*lacZ-zeo c2091*::*kan*	CFT073*lacIZ*::*cam upaC*::*lacZ-zeo c2091*::*kan*, Cam^r Zeo^r Kan^r	This study
CFT073*lacIZ upaB*::*lacZ-zeo c2411*::*kan*	CFT073*lacIZ*::*cam upaB*::*lacZ-zeo c2411*::*kan*, Cam^r Zeo^r Kan^r	This study
CFT073*lacIZ upaC*::*lacZ-zeo c2411*::*kan*	CFT073*lacIZ*::*cam upaC*::*lacZ-zeo c2411*::*kan*, Cam^r Zeo^r Kan^r	This study
CFT073*lacIZ upaB*::*lacZ-zeo c3218*::*kan*	CFT073*lacIZ*::*cam upaB*::*lacZ-zeo c3218*::*kan*, Cam^r Zeo^r Kan^r	This study
CFT073*lacIZ upaC*::*lacZ-zeo c3218*::*kan*	CFT073*lacIZ*::*cam upaC*::*lacZ-zeo c3218*::*kan*, Cam^r Zeo^r Kan^r	This study
CFT073*lacIZ upaB*::*lacZ-zeo c3244*::*kan*	CFT073*lacIZ*::*cam upaB*::*lacZ-zeo c3244*::*kan*, Cam^r Zeo^r Kan^r	This study
CFT073*lacIZ upaC*::*lacZ-zeo c3244*::*kan*	CFT073*lacIZ*::*cam upaC*::*lacZ-zeo c3244*::*kan*, Cam^r Zeo^r Kan^r	This study
CFT073*lacIZ upaB*::*lacZ-zeo c3744*::*kan*	CFT073*lacIZ*::*cam upaB*::*lacZ-zeo c3744*::*kan*, Cam^r Zeo^r Kan^r	This study
CFT073*lacIZ upaC*::*lacZ-zeo c3744*::*kan*	CFT073*lacIZ*::*cam upaC*::*lacZ-zeo c3744*::*kan*, Cam^r Zeo^r Kan^r	This study
CFT073*lacIZ upaB*::*lacZ-zeo c4864*::*kan*	CFT073*lacIZ*::*cam upaB*::*lacZ-zeo c4864*::*kan*, Cam^r Zeo^r Kan^r	This study
CFT073*lacIZ upaC*::*lacZ-zeo c4864*::*kan*	CFT073*lacIZ*::*cam upaC*::*lacZ-zeo c4864*::*kan*, Cam^r Zeo^r Kan^r	This study
CFT073*lacIZ upaB*::*lacZ-zeo c5054*::*kan*	CFT073*lacIZ*::*cam upaB*::*lacZ-zeo c5054*::*kan*, Cam^r Zeo^r Kan^r	This study
CFT073*lacIZ upaC*::*lacZ-zeo c5054*::*kan*	CFT073*lacIZ*::*cam upaC*::*lacZ-zeo c5054*::*kan*, Cam^r Zeo^r Kan^r	This study
Plasmids		
pUpaB (pOMS14)	*upaB* gene (c0426) from CFT073 in pBAD/*Myc*-HisA-*kan*, Amp^r Kan^r	This study
pUpaC (pOMS12)	*upaC* gene (c0478) from CFT073 in pBAD/*Myc*-HisA-*kan*, Amp^r Kan^r	This study
pBAD30c1701 H-NS	c1701 (H-NS) from CFT073 in pBAD30, Amp^r	37
pBR322	Amp^r Tet^r	8
pH-NS	pBR322 c1701 (H-NS) from CFT073, Amp^r	This study
pKOBEG	pSC101 ts (replicates at 30°C), *araC*, arabinose-inducible λred$\gamma\beta\alpha$ operon, Cam^r	9
pSC189	*oriT*, Π-dependent *ori*R6K, *mariner*-based transposon Tn*SC189*, Amp^r Kan^r	10

Downloaded from http://iai.asm.org/ on December 23, 2011 by INSTITUT PASTEUR-Médiathèque

containing 10^8 bacteria/ml for 2 min, followed by reintroduction of the spatula into the microfermentor. The M63B1-0.4% glucose medium flow was set at the constant rate of 0.75 ml/min. After 24 h, the biofilm formed on the spatula was resuspended in 10 ml of phosphate-buffered saline (PBS) and the optical density at 600 nm was measured for each suspension; these values directly reflect the biofilm biomass. All experiments were performed in triplicate.

ECM protein binding assays. Bacterial binding to extracellular matrix (ECM) proteins was performed in a microtiter plate enzyme-linked immunosorbent assay (ELISA) essentially as previously described (72). Microtiter plates (Maxisorp; Nunc) were coated overnight at 4°C with MaxGel human extracellular matrix (10 μg/ml) or with 2 μg of the following ECM proteins, respectively: collagen (types I to V), fibronectin, fibrinogen, laminin, elastin, heparin sulfate, human serum album, bovine serum albumin (BSA) (Sigma-Aldrich), or the glycans *N*-acetyl-D-galactosamine (NaGal), *N*-acetyl-D-glucosamine (NaGlu), or *N*-acetylneuraminic acid (NaNa). Wells were washed twice with TBS (137 mM NaCl, 10 mM Tris, pH 7.4) and then blocked with TBS-2% milk for 1 h. After being washed with TBS, 200 μl of washed and standardized (OD_{600} = 0.1) MS427(pUpaB), MS427(pUpaC), or MS427(pBAD) was added, and the plates were incubated at 37°C for 2 h. After being washed to remove nonadherent bacteria, adherent cells were fixed with 4% paraformaldehyde, washed, and incubated for 1 h with anti-*E. coli* serum (Meridian Life Sciences Inc.; catalog number B65001R) diluted 1:500 in 0.05% TBS-Tween and 0.2% milk, washed, and incubated for 1 h with a secondary anti-rabbit-conjugated horseradish peroxidase antibody (diluted 1:1,000) (Sigma-Aldrich; catalog number A6154). After a final wash, adhered bacteria were detected by adding 150 μl of 0.3 mg/ml ABTS [2,2′-azino-bis(3-ethylbenzthiazoline-6-sulfonic acid)] (Sigma-Aldrich) in 0.1 M citric acid, pH 4.3, activated with 1 μl/ml 30% hydrogen peroxide, and the absorbance was read at 405 nm. Mean absorbance readings were compared with negative-control readings of MS427(pBAD) using two-sample *t* tests within the Minitab V14 software package. *P* values of <0.05 were considered significant.

Microscopy and image analysis. UpaB or UpaC antiserum was used for immunofluorescence microscopy and immunogold electron microscopy as previously described (68, 72). Microscopic observation of biofilms and image acquisition were performed on a confocal laser-scanning microscope (LSM510 META; Zeiss) equipped with detectors and filters for monitoring of green fluorescent protein (GFP). Vertical cross sections through the biofilms were visualized using the Zeiss LSM Image Examiner. Images were further processed for display by using Photoshop software (Adobe, Mountain View, CA).

***β*-Galactosidase assays.** β-Galactosidase assays were performed essentially as previously described (43). Briefly, strains carrying *lacZ* fusions were grown on LB plates for 16 h and then inoculated into LB medium. After 16 to 18 h of growth, the culture was diluted in Z buffer (60 mM Na_2HPO_4, 40 mM NaH_2PO_4, 50 mM β-mercaptoethanol, 10 mM KCl, 1 mM $MgSO_4$, pH 7), 0.004% SDS and chloroform were added, and the samples were vortexed to permeabilize the cells. Samples were incubated at 28°C, and the reaction was initiated by the addition of ONPG (*o*-nitrophenyl-β-D-galactopyranoside). Reactions were stopped with the addition of sodium bicarbonate, and the enzymatic activity was assayed in quadruplicate for each strain by measuring the absorbance at 420 nm. In some cases, β-galactosidase activity was also observed on LB agar plates containing 5-bromo-4-chloro-3-indolyl-β-D-galactoside (X-Gal).

DNA curvature prediction and electrophoretic mobility shift assays. The *upaC* promoter region was analyzed *in silico* using bend.it, a program that enables the prediction of a curvature propensity plot calculated with DNase I-based parameters (http://hydra.icgeb.trieste.it/dna/) (73). The curvature is calculated as a vector sum of dinucleotide geometries (roll, tilt, and twist angles) and expressed as degrees per helical turn (10.5°/helical turn = 1°/bp). Experimentally tested curved motifs produce curvature values of 5 to 25°/helical turn, whereas straight motifs give values below 5°/helical turn. The *upaC* 250-bp promoter region was amplified using primers upaC.pro.ext-5+250 and upaC.pro.ext-3-1ATG, and its intrinsic curvature was assessed by comparing its electrophoretic mobility with that of an unbent marker fragment (Promega; 100-bp DNA ladder) on a 0.5% Tris-borate-EDTA (TBE), 7.5% PAGE gel at 4°C for retarded gel electrophoretic mobility.

Gel shift assays were performed essentially as previously described (3). A DNA mixture comprising an equimolar ratio of the PCR-amplified *upaC* promoter region and TaqI-SspI-digested pBR322 was incubated at room temperature for 15 min with increasing amounts of native purified H-NS protein (a gift from S. Rimsky) in 30 μl of reaction mixture containing 40 mM HEPES (pH 8), 60 mM potassium glutamate, 8 mM magnesium aspartate, 5 mM dithiothreitol, 10% glycerol, 0.1% octylphenoxypolyethoxyethanol, 0.1 mg/ml BSA (H-NS binding buffer). DNA fragments and DNA-protein complexes were resolved by gel electrophoresis (0.5% TBE, 3% MS agarose gel run at 50 V at 4°C) and visualized after staining with ethidium bromide.

Mouse model of UTI. Female C57BL/6 mice (8 to 10 weeks) were purchased from the University of Queensland Animal Facility and housed in sterile cages with *ad libitum* access to sterile water. The mouse model of UTI described previously was used for this study (54). Briefly, an inoculum of 20 μl, containing 5×10^8 CFU of bacteria in PBS (containing 0.1% India ink) was instilled directly into the bladder using a 1-ml tuberculin syringe attached to a catheter. Groups of mice were euthanized at 18 h and 5 days after challenge by cervical dislocation; bladders were then excised aseptically, weighed, and homogenized in PBS. Bladder homogenates were serially diluted in PBS and plated onto LB agar for colony counts. Competitive mixed-infection assays were performed as described above except that mice were inoculated with a 50:50 mixture of CFT073^{amp} and CFT073*upaB* or CFT073*upaC* grown in the absence of antibiotics. The two strains were differentiated by their resistance to ampicillin (CFT073^{amp}) and zeocin (CFT073*upaB*) or kanamycin (CFT073*upaC*) to enable differential colony counts of the recovered bacteria. The output ratios were normalized to the input ratios to determine the competitive index ([mutant ouput/wild-type ouput]/[mutant input/wild-type input]). For competitive infections, significance was determined using the Wilcoxon rank-sum test on $\log_{10}$-transformed fitness indices against a hypothetical median of 0 ($\log_{10}1 = 0$) using GraphPad Prism 5. For single infections, the median numbers of bacterial CFU were compared using the nonparametric Mann-Whitney test within the Minitab V14 software package. *P* values of <0.05 were considered significant.

Statistical analysis. The prevalences of the *upaB* and *upaC* genes in uropathogenic and nonpathogenic *E. coli* strains were compared using Fisher's exact test.

RESULTS

Bioinformatic analysis of the UpaB and UpaC AT proteins from UPEC CFT073. Eleven putative AT-encoding genes have been identified in the sequenced genome of the prototype UPEC strain CFT073 (1, 50). In order to investigate the functionality of UpaB and UpaC, we performed a bioinformatic analysis of these hypothetical proteins. Analysis of the 770-amino-acid UpaB and the 995-amino-acid UpaC sequence using the Conserved Domain Database (CDD) (40, 41) and the Simple Modular Architecture Design Tool (SMART) (39) identified a pertactin-like passenger domain (cl00185) followed by an AT β-domain (cl002365) in the C-terminal region of both proteins. The predicted β-domain sequence begins at amino acid 500 for UpaB and amino acid 725 for UpaC. Further analysis with SignalP (6) identified a characteristic signal peptide for both proteins (31 amino acids in length for UpaB and 27 amino acids in length for UpaC). We also detected sequence similarity to the pectin lyase-like superfamily within the passenger (α) domain of UpaB and UpaC using InterProScan (82). The pectin lyase-like superfamily sequence has a predominant secondary structure of right-handed parallel β-helix topology.

Downloaded from http://iai.asm.org/ on December 23, 2011 by INSTITUT PASTEUR-Médiathèque

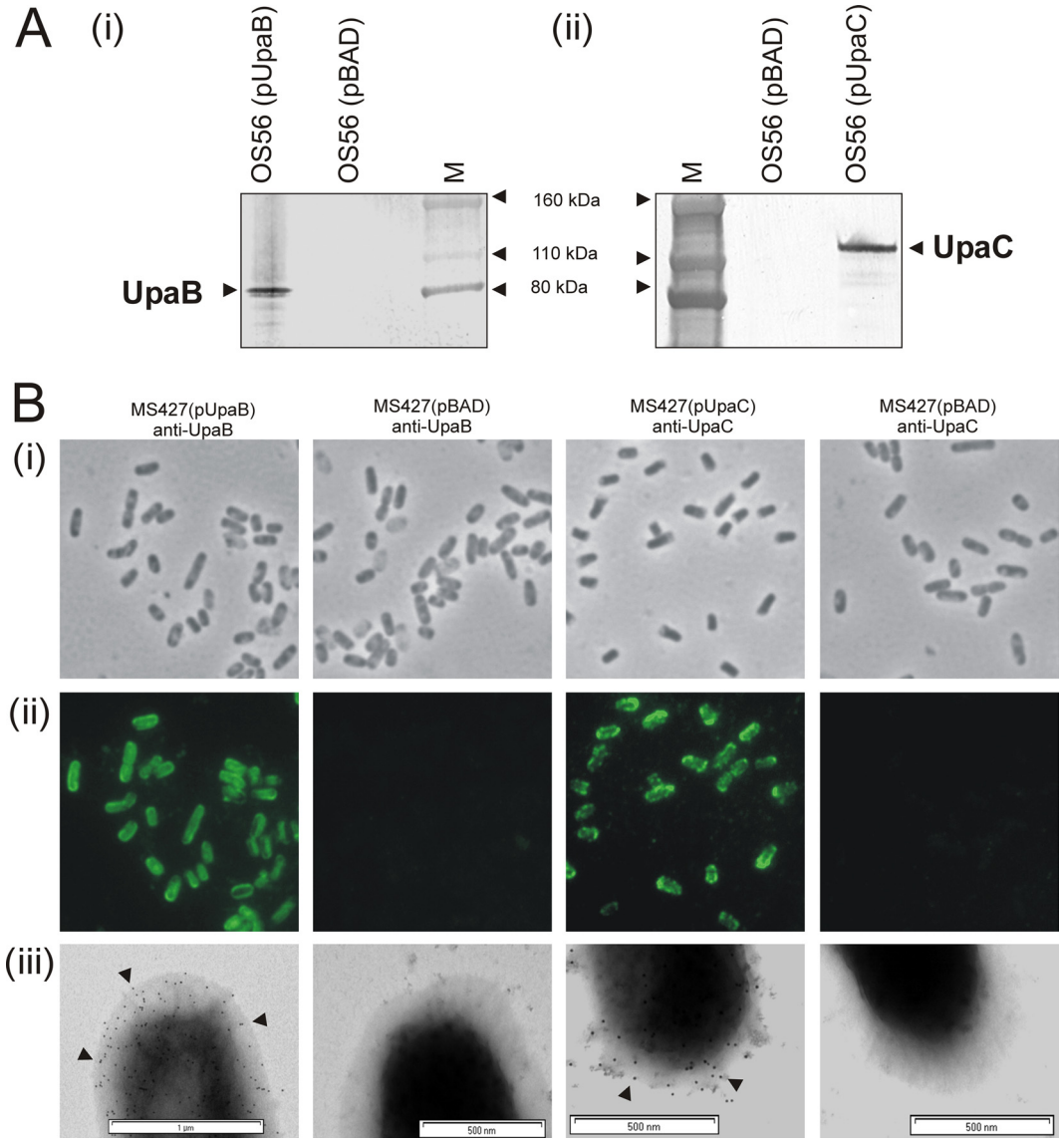

FIG 1 (A) Western blot analysis of UpaB and UpaC performed using whole-cell lysates prepared from *E. coli* grown in the presence of 0.2% arabinose. (i) OS56(pUpaB), OS56(pBAD); (ii) OS56(pUpaC), OS56(pBAD). Lane M, Novex Sharp molecular weight marker. (B) Phase contrast (i), immunofluorescence (ii), and immunogold electron microscopy (iii) using UpaB-specific antiserum against cells of *E. coli* strains MS427(pUpaB) and MS427(pBAD) or UpaC antiserum against cells of *E. coli* strains MS427(pUpaC) or MS427(pBAD). Cells were grown in the presence of 0.2% arabinose. Overnight cultures were fixed and incubated with anti-UpaB or anti-UpaC serum, respectively, followed by incubation with goat anti-rabbit IgG coupled to Alexa Fluor 488 for immunofluorescence or protein A-gold (10 nm) conjugate. Gold particles were present on the surface of *E. coli* MS427(pUpaB) and MS427(pUpaC) but not on that of the MS427(pBAD) control strain.

Prevalence of the AT-encoding genes in UPEC. The prevalences of the *upaB* and *upaC* genes were assessed by PCR screening of uropathogenic and nonpathogenic *E. coli* strains obtained from both the ECOR collection (48) and our own laboratory collection. The *upaB* and *upaC* genes are common among UPEC strains (58% [21/36] and 47% [17/36], respectively) and nonpathogenic *E. coli* strains (42% [26/62] and 34% [21/62], respectively). There was no significant difference between the presence of the genes in UPEC and nonpathogenic *E. coli*.

Cloning and expression of AT-encoding genes from UPEC CFT073. The *upaB* (c0426) and *upaC* (c0478) genes were PCR amplified and cloned as a transcriptional fusion downstream of the tightly regulated *araBAD* promoter in the pBAD/*Myc*-HisA expression vector to generate the plasmids pUpaB (pOMS14) and pUpaC (pOMS12), respectively. To demonstrate expression of the UpaB and UpaC proteins, plasmids pUpaB and pUpaC were transformed into the *E. coli* K-12 *flu* mutant strains MS427 and OS56, respectively. *E. coli* MS427 contains a mutation in the Ag43-encoding *flu* gene and is unable to mediate cell aggregation and biofilm formation (52), while OS56 is a derivative of MS427 that has been tagged at the λ-attachment site with *gfp* (64). In the case of UpaB, Western blot analysis using a UpaB-specific antiserum resulted in the detection of a band corresponding to the full-length UpaB protein (80.1 kDa) in whole-cell lysates prepared from *E. coli* OS56(pUpaB) following induction with arabinose (Fig. 1A). Likewise, in the case of UpaC, Western blot analysis

Downloaded from http://iai.asm.org/ on December 23, 2011 by INSTITUT PASTEUR-Médiathèque

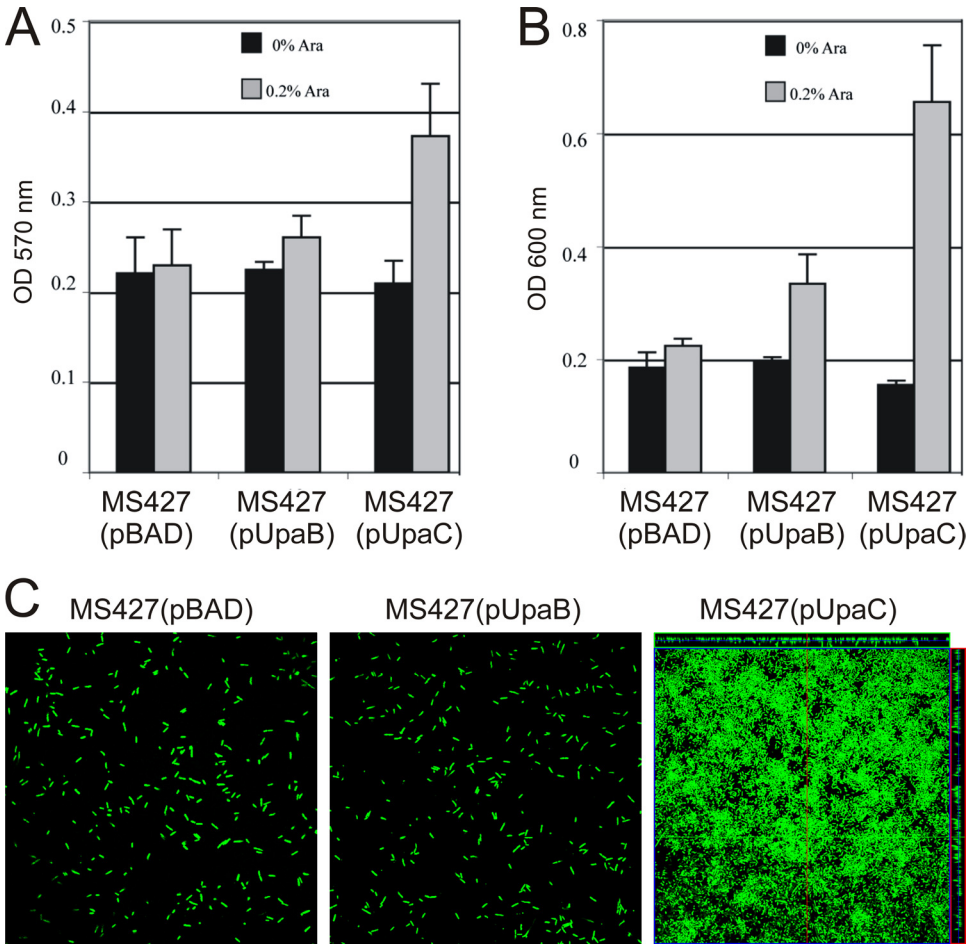

FIG 2 Biofilm formation by *E. coli* OS56 cells harboring plasmids expressing UpaB and UpaC. The effect of AT expression on biofilm formation was assessed in *E. coli* OS56 (MG1655Δ*flu*, Gfp+) cells containing the following plasmids pBAD, pUpaB, or pUpaC. All strains were grown in the presence of 0.2% arabinose to induce AT protein expression. Three assays were used: (A) static biofilm formation in polystyrene microtiter plates, (B) dynamic biofilm formation in a microfermentor system, and (C) dynamic biofilm formation using a flow chamber model. In the dynamic-flow-chamber biofilm development was monitored by confocal scanning laser microscopy after 15 h. The images are representative horizontal sections collected within each biofilm and vertical sections (to the right of and above each larger panel, representing the *yz* plane and the *xz* plane, respectively) at the positions indicated by the red and green lines. *E. coli* MS427(pUpaC) produced a biofilm with a significant increase in total biovolume, substratum coverage and mean thickness compared to the vector control strain at 15 h postinoculation (COMSTAT). In the microfermentor assay, UpaC also promoted significant biofilm growth compared to the vector control strain (unpaired *t* test with Welch′s correction $P < 0.05$).

using a UpaC antiserum resulted in the detection of a band of 120 kDa (slightly larger than the predicted 107-kDa molecular mass of UpaC) in whole-cell lysates prepared from *E. coli* OS56 (pUpaC) following induction with arabinose (Fig. 1A). No processing or cleavage of the respective mature passenger and translocation domain from UpaB or UpaC was observed in whole-cell lysates or following brief heat treatment of the cells at 60°C for 3 min (data not shown).

UpaB and UpaC are located at the bacterial cell surface. To examine if the UpaB and UpaC AT proteins were localized to the outer membrane, immunofluorescence microscopy was performed (Fig. 1B). UpaB and UpaC antiserum readily reacted with *E. coli* MS427(pUpaB) and MS427(pUpaC), respectively, following induction with arabinose during growth in LB broth. Thus, UpaB and UpaC were effectively translocated to the cell surface. No reaction was seen with *E. coli* MS427(pBAD) cells. Surface localization of UpaB and UpaC was confirmed using immunogold labeling and electron microscopy (Fig. 1B). *E. coli* MS427(pUpaB) and MS427(pUpaC) cells clearly displayed surface labeling with gold particles following incubation with UpaB or UpaC antiserum compared to *E. coli* MS427(pBAD) cells. Thus, the *upaB* and *upaC* genes are functional and encode proteins located at the cell surface in *E. coli*.

Phenotypic properties of UpaB and UpaC. AT proteins are frequently associated with aggregation, cell adherence, adhesion to ECM proteins, and biofilm formation. The overexpression of UpaB and UpaC in *E. coli* OS56 did not result in aggregation or adherence to T24 epithelial cells, HeLa cells, or shed human uroepithelial cells. However, when we assessed the ability to form a biofilm in a static, nontreated polystyrene microtiter plate model, UpaC, but not UpaB, promoted biofilm formation after growth in LB medium (*t* test, $P < 0.01$) (Fig. 2A). Next, we tested the ability of the AT proteins to promote biofilm formation in dynamic conditions using the microfermentor and continuous flow chamber model systems, the latter allowing us to monitor bacterial distribution within an evolving biofilm at the single-cell level due to the

Downloaded from http://iai.asm.org/ on December 23, 2011 by INSTITUT PASTEUR-Médiathèque

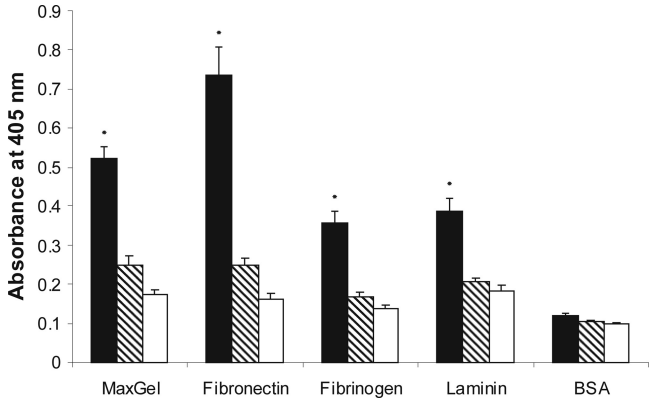

FIG 3 UpaB mediates attachment to a range of ECM proteins in an ELISA-based binding assay. Black bars, *E. coli* MS427(pUpaB); hatched bars, *E. coli* MS427(pUpaC); white bars, *E. coli* MS427(pBAD). Results represent averages of results from 3 independent experiments + standard errors of the means (SEM). Mean absorbance readings were compared with negative-control readings MS427(pBAD).

combination of *gfp*-tagged cells and confocal laser-scanning microscopy. UpaC promoted significant biofilm growth in both the flow cell and microfermentor assays (unpaired *t* test with Welch's correction, $P < 0.05$) (Fig. 2B and C). Thus, UpaC represents a UPEC AT protein that promotes biofilm growth.

Next, we used an ELISA-based method to test the abilities of UpaB and UpaC to mediate adherence to MaxGel, a commercially available mixture of ECM components, including collagens, laminin, fibronectin, tenascin, elastin, a number of proteoglycans, and glycosaminoglycans. UpaB (but not UpaC) promoted significant binding to MaxGel (Fig. 3), and this prompted us to examine binding in more detail by testing a range of different ECM proteins. UpaB promoted binding to fibronectin, fibrinogen, and laminin but not to BSA (negative control) (Fig. 3) or to collagen type I, type II, type III, type IV, and type V, elastin, heparin sulfate, human serum album, or the glycans *N*-acetyl-D-galactosamine (NaGal), *N*-acetyl-D-glucosamine (NaGlu), and *N*-acetylneuraminic acid (NaNa) (data not shown). Therefore, UpaB represents a UPEC AT protein that promotes specific binding to some ECM proteins.

The UpaB protein is expressed by CFT073. To determine whether the UpaB and UpaC proteins are expressed by *E. coli* CFT073, we constructed isogenic deletion mutants of *upaB* and *upaC*, respectively, using λ-red-mediated homologous recombination of linear DNA (these mutants are referred to as CFT073*upaB* and CFT073*upaC*, respectively). Examination of whole-cell lysates prepared from these isogenic strains following growth in LB broth by Western blotting showed expression of UpaB (but not UpaC) in *E. coli* CFT073 (Fig. 4A). This was, however, not sufficient to allow detection of UpaB at the cell surface of CFT073 by immunofluorescence (Fig. 5A). Nevertheless, complementation of CFT073*upaB* with plasmid pUpaB restored the ability of this strain to produce detectable levels of UpaB at the cell surface (Fig. 5A). Western blot analysis did not show expression of UpaC from CFT073 (Fig. 4B). Accordingly, UpaC could not be detected at the cell surface of CFT073 by immunofluorescence (Fig. 5B). This was not caused by a defect in the stability of the protein, as complementation of CFT073*upaC* with pUpaC resulted in detection of UpaC (Fig. 5B). In addition, we detected surface localization of both UpaB and UpaC in UpaB/UpaC overexpression strains constructed by chromosomal insertion of the inducible RExBAD expression cassette and a λP_R constitutive promoter (13, 55) in front of each open reading frame, respectively (CFT073RexBAD*upaB* and CFT073RexBAD*upaC*, CFT073PcL*upaB* and CFT073PcL*upaC*) (Fig. 5).

The H-NS protein is a repressor of UpaC. To investigate the genetic basis of repression of *upaC* and compare this to *upaB*, we inserted an *lacZ* reporter as a transcriptional fusion to the promoters of *upaB* and *upaC* on the chromosome of CFT073*lacI-Z* to generate the CFT073*lacI-Z upaB*::*lacZ-zeo* and CFT073*lacI-Z upaC*::*lacZ-zeo* strains. When grown on X-Gal plates, all CFT073*lacI-Z upaB*::*lacZ-zeo* colonies were blue (indicating transcription) and all CFT073*lacI-Z upaC*::*lacZ-zeo* colonies were very faint blue (indicating very low levels of transcription). No color heterogeneity was observed among the CFT073*lacI-Z upaB*::*lacZ-zeo* and CFT073*lacI-Z upaC*::*lacZ-zeo* colonies, indicating that expression of UpaB and UpaC is not subjected to phase variation.

Subsequently, we created specific gene deletions by λ-red-mediated homologous recombination in a panel of defined/putative *E. coli* CFT073 regulatory genes: c0421 (*virF* like), c1699 (*rpoS*), c1701 (*hns*), c2091 (*virF* like), c2411 (*hns* like), c3218 (*stpA*), c3244 (*luxS* AI-2), c3744 (*virF* like), c4864 (*cpxR* periplasmic stress), and c5054 (*soxR* oxidative stress) in CFT073*lacI-Z upaB*::*lacZ-zeo* and CFT073*lacI-Z upaC*::*lacZ-zeo* strains. Each of these mutants was then assayed for β-galactosidase activity to assess the effect of these regulators on transcription from the *upaB* or *upaC* promoter (data not shown). No regulators of *upaB* were identified (data not shown). However, H-NS was identified as a repressor of *upaC*; the CFT073*lacI-Z upaC*::*lacZ-zeo hns* mutant exhibited a 20-fold increase in β-galactosidase activity compared to that of the CFT073*lacI-Z upaC*::*lacZ-zeo* mutant (Fig. 4C). An independent experiment employing random mariner transposon mutagenesis resulted in the generation of six blue colonies, all of which possessed significantly increased β-galactosidase activity due to the inactivation of *hns* and thus confirmed these observations (data not shown). We also complemented the CFT073*lacI-Z upaC*::*lacZ-zeo hns* mutant with an *hns*-containing plasmid (pH-NS), and this resulted in a significant reduction in the expression of *upaC* (Fig. 4C). Thus, UpaC is repressed by H-NS.

The H-NS protein represses *upaC* transcription in CFT073. To confirm the above-mentioned results, an *hns* isogenic mutant was constructed in CFT073 and examined via Western blot analysis. Loss of H-NS from CFT073 resulted in the appearance of a band representing UpaC, which migrated at the same size as UpaC from OS56(pUpaC) (Fig. 1A). However, no expression of UpaC was observed in a CFT073*upaC hns* double mutant (Fig. 4B). This H-NS specific repression of UpaC was not observed for UpaB, which was detected in wild-type CFT073 and a CFT073 *hns* mutant (Fig. 4A). Taken together, these results demonstrate that H-NS negatively regulates the expression of UpaC.

H-NS binds to the promoter region of *upaC*. H-NS binds to intrinsically curved regions of DNA. An *in silico*-generated curvature-propensity plot calculated with DNase I-based parameters suggested that the promoter region of *upaC* may adopt a curved conformation (Fig. 4D). To experimentally demonstrate this curvature, a 250-bp PCR product containing the predicted *upaC* promoter region was generated and examined by polyacrylamide gel electrophoresis at 4°C. This method has been used previously to demonstrate DNA curvature (71, 81). Indeed, the 250-bp *upaC* promoter region displayed a slightly retarded gel

Downloaded from http://iai.asm.org/ on December 23, 2011 by INSTITUT PASTEUR-Médiathèque

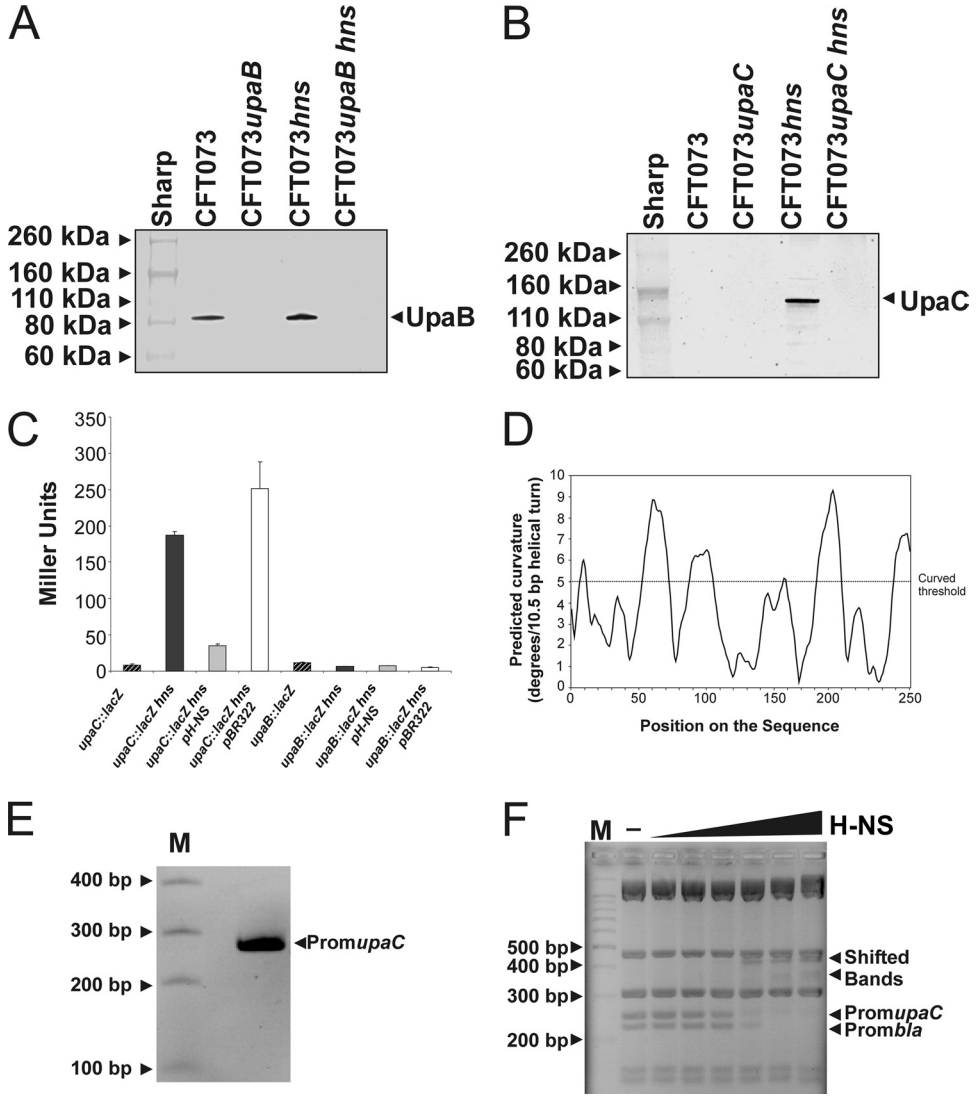

FIG 4 The H-NS protein is a repressor of UpaC. (A) Western blot analysis of UpaB using whole-cell lysates; (B) Western blot analysis of UpaC using whole-cell lysates; (C) beta-galactosidase assay of *upaB*::*lacZ-zeo* and *upaC*::*lacZ-zeo* fusions; (D) curvature propensity plots showing predicted regions of curved DNA in the 250-bp *upaC* promoter. (E) Curved DNA PAGE gel of the amplified 250-bp *upaC* promoter at 4°C. Migration of this band is slightly retarded in the gel, suggesting that the DNA is curved. (F) Electrophoretic band shift of the amplified 250-bp *upaC* promoter and the *bla* promoter from digest pBR322 DNA. The pBR322 fragments not containing the *bla* promoter were not influenced by the increasing concentrations of (0.05, 0.1, 0.2, 0.5, 1, and 2 μM) H-NS. Images depict representative gels from at least two independent experiments.

electrophoretic mobility compared to that of noncurved DNA standards (Fig. 4E). In order to investigate whether H-NS influences gene expression by direct binding to the curved promoter region of *upaC*, we performed electrophoretic mobility shift assays. The 250-bp PCR product was mixed with TaqI-SspI-digested pBR322 DNA (which contains the *bla* promoter and has been previously shown to be bound by H-NS) and was incubated with increasing concentrations of purified H-NS protein and subsequently visualized by gel electrophoresis. The 250-bp *upaC* promoter region and the fragment containing the *bla* promoter were retarded in mobility by the addition of 0.5 μM H-NS (Fig. 4F). The pBR322 fragments not containing the *bla* promoter were not influenced by H-NS at these concentrations, indicating that H-NS binds with specificity. These results suggest that H-NS binds to the regulatory region of *upaC* by recognizing a DNA region within 250 bp 5′ of the ATG translation start codon.

Deletion of *upaB* from CFT073 reduces colonization of the mouse bladder in a mixed-infection competition assay. To assess the role of UpaB and UpaC on virulence, we examined the ability of CFT073, CFT073*upaB*, and CFT073*upaC* to survive in competitive colonization experiments. The strains had identical growth rates in LB broth and did not display any difference with respect to type 1 fimbriae production (as assessed by yeast cell agglutination and an *fim* switch orientation PCR) (data not shown). Mice were coinoculated with CFT073 and CFT073*upaB* or CFT073 and CFT073*upaC* strains in a 1:1 ratio. In this assay, CFT073*upaB* was significantly outcompeted by CFT073 in the bladder of infected mice ($P = 0.014$) (Fig. 6A). No difference in colonization was observed between CFT073 and CFT073*upaC* (Fig. 6A).

Deletion of *upaB* from CFT073 reduces colonization of the mouse bladder in single-infection experiments. To further assess the role of UpaB on virulence, we examined the ability of

Downloaded from http://iai.asm.org/ on December 23, 2011 by INSTITUT PASTEUR-Médiathèque

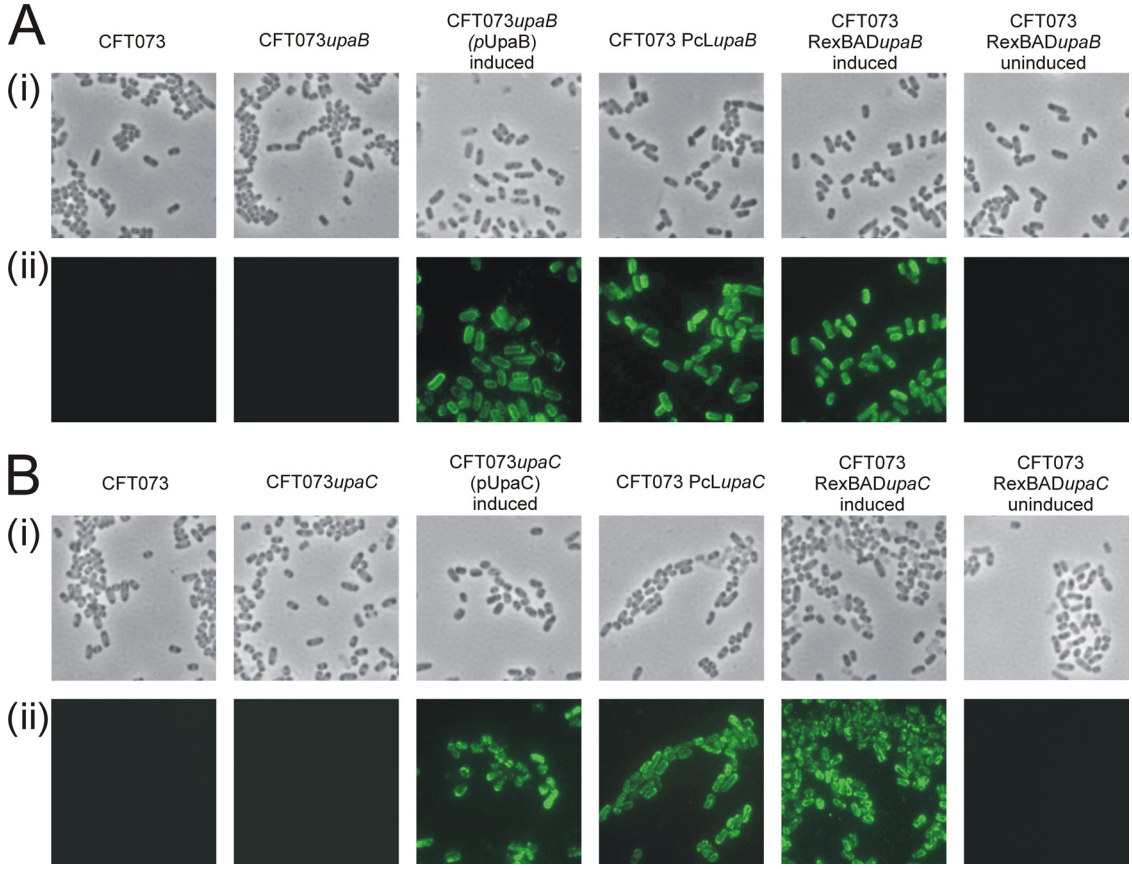

FIG 5 (A) Phase-contrast (i) or immunofluorescence (ii) microscopy employing UpaB-specific antiserum against cells of *E. coli* strains as specified; (B) phase-contrast (i) or immunofluorescence (ii) microscopy using UpaC antiserum against cells of *E. coli* strains as specified. Strains were grown in the presence of 0.2% arabinose and labeled as induced where applicable. Overnight cultures were fixed and incubated with anti-UpaB or anti-UpaC serum followed by incubation with goat anti-rabbit IgG coupled to Alexa Fluor 488. A positive reaction indicating surface localization of UpaB or UpaC was detected only for the overexpressing strains.

CFT073 and CFT073*upaB* to survive in the mouse urinary tract in single-infection experiments employing a short (1-day)- and long (5-day)-term protocol. We observed a significant reduction in colonization of the bladder by the CFT073*upaB* mutant ($P < 0.001$; Fig. 6B) at day 1 postinfection. However, by day 5 postinfection, equivalent bacterial loads were recovered for CFT073 and CFT073*upaB* (Fig. 6C). No significant colonization of the kidneys was observed for either strain; this is consistent with previous data from our laboratory using C57BL/6 mice (68, 72).

DISCUSSION

UPEC strains produce a range of fimbrial and nonfimbrial adhesins that play a role in virulence and contribute to persistent infection of the urinary tract. Some UPEC fimbrial adhesins, including type 1 and P fimbriae, have been well characterized with respect to their expression, regulation, receptor-binding target, and role in virulence. Of the nonfimbrial adhesins, the AT family of proteins represents another group of virulence factors that contribute to adhesion, invasion, and biofilm formation. Although UPEC strains possess multiple AT-encoding genes, very little is known about the function of their products and only Ag43, UpaG, Sat, and UpaH have been associated with virulence (1, 21, 22, 69, 72). Here, we characterize the UpaB and UpaC AT proteins from CFT073; we demonstrate that UpaB mediates binding to ECM proteins and contributes to early colonization of the mouse bladder, while UpaC contributes to *in vitro* biofilm formation.

Eleven putative AT-encoding genes have been identified in the sequenced genome of the prototype UPEC strain CFT073 (1, 50). In this study, we cloned and characterized the *upaB* and *upaC* AIDA-I-type AT-encoding genes from CFT073. The *upaB* gene is present in all available UPEC genomes but absent or disrupted in all diarrheagenic *E. coli* genomes (77), suggesting that it may contribute to UPEC virulence. The *upaC* gene is disrupted in the commensal *E. coli* strains MG1655, DH1, and HS. While there was no significant difference in the prevalence of the *upaB* and *upaC* genes in UPEC and nonpathogenic *E. coli*, our data suggest that their presence is associated with gene acquisition or loss mediated by mobile genetic elements.

UpaB and UpaC both contain a predicted signal sequence, a pertactin-like domain, and an AT β-domain that is common to all AT proteins. The passenger domain possesses sequence similarity to the pectin lysase-like superfamily and contains an extensive β-sheet secondary structure as predicted by the fold recognition program I-TASSER (83). It is therefore likely that the passenger domain of UpaB and UpaC comprises a β-helix structure akin to that proposed for the majority of other AT proteins (33).

Several studies have demonstrated that the intimate cell-cell

Downloaded from http://iai.asm.org/ on December 23, 2011 by INSTITUT PASTEUR-Médiathèque

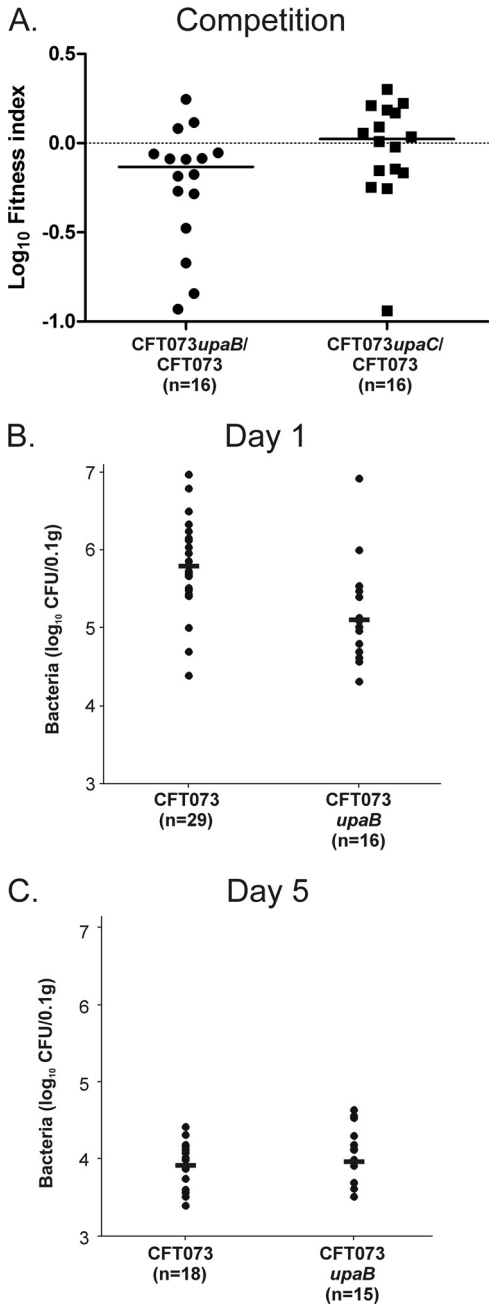

FIG 6 Mouse UTI assays. (A) Competitive mixed-infection experiment employing a 1:1 mixture of *E. coli* CFT073^{amp}/CFT073*upaB* and *E. coli* CFT073^{amp}/CFT073*upaC*. Total CFU were enumerated from the bladders of infected mice on selective medium to differentiate between *E. coli* CFT073^{amp}/CFT073*upaB* and *E. coli* CFT073^{amp}/CFT073*upaC*. Each symbol represents the Log_{10} fitness index calculated for each individual mouse, and the median is represented by a horizontal line. A Log_{10} fitness index below 0 (shown by the dashed line) indicates that the *upaB* mutant is at a competitive disadvantage ($P = 0.014$). (B and C) Single-infection assay employing *E. coli* CFT073 and CFT073*upaB*. Data for individual mice are expressed as the Log_{10} of total CFU per 0.1 g of bladder tissue at day 1 (B) and day 5 (C) postinfection. The number of mice used for each experiment (n) is indicated. The data represent a compilation of the results from two individual experiments. Medians are indicated by a solid line. *E. coli* CFT073 was recovered from the bladder of infected mice at day 1 postinfection in significantly higher numbers than CFT073*upaB* ($P < 0.001$). No statistical difference in the number of *E. coli* CFT073 and CFT073*upaB* was observed at day 5 postinfection.

contact required for AT adhesin interaction can be physically blocked by the expression of larger surface structures, such as fimbriae, flagella, lipopolysaccharide (LPS), and the capsule (4, 26, 60, 61, 64, 68, 70). Our strategy to study the function of UpaB and UpaC involved the use of two host strains, MG1655*flu* and UPEC CFT073. The MG1655*flu* strain (and its GFP-positive derivative OS56) are well characterized and represent an ideal background to assess the function of AT adhesins (64). The surface expression of UpaC (but not UpaB) in this background significantly increased biofilm formation, while UpaB (but not UpaC) mediated adherence to several ECM proteins, including fibronectin, fibrinogen, and laminin. The lack of UpaC-mediated binding to laminin was in contrast to the previously reported binding characteristics of a closely related homologue, EhaB from enterohemorrhagic *E. coli* (EHEC) (75). Although EhaB and UpaC share 62.1% amino acid sequence identity and are detected with the same polyclonal EhaB antiserum, the molecular basis for this difference in function remains to be elucidated.

Immunodetection of the UpaB and UpaC proteins revealed that while UpaB could be detected in whole-cell extracts of CFT073, the UpaC protein was not detected in whole-cell extracts of CFT073 prepared under the same conditions. The difference between the β-galactosidase activity measured from the *upaB lacZ* transcriptional fusion strain and the level of UpaB detected in CFT073 by Western blot analysis may be due to mRNA stability or posttranscriptional factors that affect protein stability. H-NS is a histone-like DNA binding protein that represses multiple virulence factors in UPEC (45), and our results demonstrated that H-NS also acts as a repressor of *upaC* transcription, most likely through direct binding to its promoter region. H-NS was shown to bind to a region comprising the 250 bp upstream of the *upaC* open reading frame. Modulating the expression of the *hns* gene may well be a mechanism evolved by UPEC and other *E. coli* strains to control the expression of various virulence factors, including adhesins. It is possible that the transcription of *upaC* is coordinated with other H-NS repressed genes; for example, several cryptic *E. coli* chaperone-usher fimbrial genes were also recently shown to be repressed by H-NS (37). In contrast to *upaC*, targeted mutagenesis strategies did not indicate that the transcription of *upaB* is regulated by H-NS.

While *upaC* expression was repressed in CFT073 during *in vitro* growth, analysis of the data deposited in the Array Express database examining the transcriptome of the asymptomatic urinary tract colonizer *E. coli* 83972 identified upregulation of *upaC* transcription during biofilm formation in human urine (25), suggesting that UpaC is expressed under conditions similar to those encountered in the urinary tract. Additionally, Hagan et al. recently published the first transcriptome analysis for UPEC collected from the urine of patients with symptomatic UTI and compared this to the transcriptome of the same strains grown *in vitro* (24). Analysis of the data deposited in the GEO series database revealed that transcripts for *upaB* and *upaC* were detected in some UPEC strains, suggesting that these genes are transcribed during human UTI. We observed a significant difference in bladder colonization between CFT073 and CFT073*upaB* in a competitive mixed-infection assay and at day 1 postinfection in a single-infection assay, strongly suggesting that expression of UpaB is associated with early colonization of the mouse bladder. In contrast, we did not observe any difference between CFT073 and CFT073*upaB* at day 5 postinfection.

Downloaded from http://iai.asm.org/ on December 23, 2011 by INSTITUT PASTEUR-Médiathèque

In the murine UTI model, UPEC colonization of the bladder is associated with the formation of intracellular bacterial communities (IBCs) within superficial umbrella cells (2). IBCs possess biofilm-like properties and are comprised of compact cell clusters encased in a polysaccharide matrix. IBC formation creates a quiescent state that may be associated with long-term persistence in the bladder (17, 47). Two phase-variable cell surface factors associated with biofilm formation, type 1 fimbriae and Ag43, are expressed by UPEC within IBCs (2). We did not observe any evidence of phase-variable expression of UpaB or UpaC. However, given that UpaC promoted biofilm formation and UpaB promoted adherence to several ECM proteins, it is possible that both UpaB and UpaC contribute to this phenotype.

A number of AT proteins have now been shown to contribute to UPEC virulence. Ag43, UpaB, and UpaH contribute to colonization of the mouse bladder, albeit at different stages of infection. The UpaB and UpaG AT proteins mediate adherence to ECM proteins, while UpaG is also associated with adherence to bladder epithelial cells. In addition, the majority of these AT proteins are associated with biofilm formation, with Ag43 also contributing to IBC formation. The expression of these proteins may be coordinated with other larger surface structures, such as the capsule, O antigen, flagella, and fimbriae, to mediate their affect on the ability of UPEC to colonize different niches.

ACKNOWLEDGMENTS

We thank Laura Zanichelli, Tim J. Wells, Chelsea Stewart, and Barbara Arnts for expert assistance, as well as Sylvie Rimsky for providing the purified native H-NS protein and Per Klemm for providing strain CFT073^{amp}.

This work was supported by grants from the Australian National Health and Medical Research Council (631654), the Australian Research Council (DP1097032), the University of Queensland, the Institut Pasteur, the CNRS URA 2172, the Network of Excellence EuroPathoGenomics, and the European Community (LSHB-CT-2005-512061).

M.A.S. is supported by an ARC Future Fellowship, and J.V. was a Marie-Curie Fellow.

REFERENCES

1. **Allsopp LP, et al.** 2010. UpaH is a newly identified autotransporter protein that contributes to biofilm formation and bladder colonization by uropathogenic *Escherichia coli* CFT073. Infect. Immun. **78**:1659–1669.
2. **Anderson GG, et al.** 2003. Intracellular bacterial biofilm-like pods in urinary tract infections. Science **301**:105–107.
3. **Beloin C, Dorman C.** 2003. An extended role for the nucleoid structuring protein H-NS in the virulence gene regulatory cascade of *Shigella flexneri.* Mol. Microbiol. **47**:825–838.
4. **Beloin C, et al.** 2006. The transcriptional antiterminator RfaH represses biofilm formation in *Escherichia coli.* J. Bacteriol. **188**:1316–1331.
5. **Beloin C, et al.** 2004. Global impact of mature biofilm lifestyle on *Escherichia coli* K-12 gene expression. Mol. Microbiol. **51**:659–674.
6. **Bendtsen JD, Nielsen H, von Heijne G, Brunak S.** 2004. Improved prediction of signal peptides: SignalP3.0. J. Mol. Biol. **340**:783–795.
7. **Bertani G.** 1951. Studies on lysogenesis. I. The mode of phage liberation by lysogenic *Escherichia coli.* J. Bacteriol. **62**:293–300.
8. **Bolivar F, et al.** 1977. Construction and characterization of new cloning vehicles. II. A multipurpose cloning system. Gene **2**:95–113.
9. **Chaveroche MK, Ghigo JM, d'Enfert C.** 2000. A rapid method for efficient gene replacement in the filamentous fungus *Aspergillus nidulans.* Nucleic Acids Res. **28**:E97.
10. **Chiang SL, Rubin EJ.** 2002. Construction of a mariner-based transposon for epitope-tagging and genomic targeting. Gene **296**:179–185.
11. **Connell I, et al.** 1996. Type 1 fimbrial expression enhances *Escherichia coli* virulence for the urinary tract. Proc. Natl. Acad. Sci. U. S. A. **93**: 9827–9832.
12. **Da Re S, Ghigo JM.** 2006. A CsgD-independent pathway for cellulose production and biofilm formation in *Escherichia coli.* J. Bacteriol. **188**: 3073–3087.
13. **Da Re S, Le Quere B, Ghigo JM, Beloin C.** 2007. Tight modulation of *Escherichia coli* bacterial biofilm formation through controlled expression of adhesion factors. Appl. Environ. Microbiol. **73**:3391–3403.
14. **Datsenko KA, Wanner BL.** 2000. One-step inactivation of chromosomal genes in *Escherichia coli* K-12 using PCR products. Proc. Natl. Acad. Sci. U. S. A. **97**:6640–6645.
15. **Derbise A, Lesic B, Dacheux D, Ghigo JM, Carniel E.** 2003. A rapid and simple method for inactivating chromosomal genes in *Yersinia.* FEMS Immunol. Med. Microbiol. **38**:113–116.
16. **Donnelly MI, et al.** 2006. An expression vector tailored for large-scale, high-throughput purification of recombinant proteins. Protein Expr. Purif. **47**:446–454.
17. **Eto DS, Sundsbak JL, Mulvey MA.** 2006. Actin-gated intracellular growth and resurgence of uropathogenic *Escherichia coli.* Cell. Microbiol. **8**:704–717.
18. **Ferrieres L, Hancock V, Klemm P.** 2007. Specific selection for virulent urinary tract infectious *Escherichia coli* strains during catheter-associated biofilm formation. FEMS Immunol. Med. Microbiol. **51**:212–219.
19. **Foxman B.** 2002. Epidemiology of urinary tract infections: incidence, morbidity, and economic costs. Am. J. Med. **113 Suppl. 1A**:5S–13S.
20. **Ghigo JM.** 2001. Natural conjugative plasmids induce bacterial biofilm development. Nature **412**:442–445.
21. **Guyer DM, Henderson IR, Nataro JP, Mobley HL.** 2000. Identification of Sat, an autotransporter toxin produced by uropathogenic *Escherichia coli.* Mol. Microbiol. **38**:53–66.
22. **Guyer DM, Radulovic S, Jones FE, Mobley HL.** 2002. Sat, the secreted autotransporter toxin of uropathogenic *Escherichia coli*, is a vacuolating cytotoxin for bladder and kidney epithelial cells. Infect. Immun. **70**: 4539–4546.
23. **Guzman LM, Belin D, Carson MJ, Beckwith J.** 1995. Tight regulation, modulation, and high-level expression by vectors containing the arabinose PBAD promoter. J. Bacteriol. **177**:4121–4130.
24. **Hagan EC, Lloyd AL, Rasko DA, Faerber GJ, Mobley HL.** 2010. *Escherichia coli* global gene expression in urine from women with urinary tract infection. PLoS Pathog. **6**:e1001187.
25. **Hancock V, Klemm P.** 2007. Global gene expression profiling of asymptomatic bacteriuria *Escherichia coli* during biofilm growth in human urine. Infect. Immun. **75**:966–976.
26. **Hasman H, Chakraborty T, Klemm P.** 1999. Antigen-43-mediated autoaggregation of *Escherichia coli* is blocked by fimbriation. J. Bacteriol. **181**:4834–4841.
27. **Henderson IR, Cappello R, Nataro JP.** 2000. Autotransporter proteins, evolution and redefining protein secretion. Trends Microbiol. **8**:529–532.
28. **Henderson IR, Navarro-Garcia F, Desvaux M, Fernandez RC, Ala'Aldeen D.** 2004. Type V protein secretion pathway: the autotransporter story. Microbiol. Mol. Biol. Rev. **68**:692–744.
29. **Heydorn A, et al.** 2000. Quantification of biofilm structures by the novel computer program COMSTAT. Microbiology **146**:2395–2407.
30. **Ieva R, Bernstein HD.** 2009. Interaction of an autotransporter passenger domain with BamA during its translocation across the bacterial outer membrane. Proc. Natl. Acad. Sci. U. S. A. **106**:19120–19125.
31. **Jones CH, et al.** 1995. FimH adhesin of type 1 pili is assembled into a fibrillar tip structure in the *Enterobacteriaceae.* Proc. Natl. Acad. Sci. U. S. A. **92**:2081–2085.
32. **Jose J, Jahnig F, Meyer TF.** 1995. Common structural features of IgA1 protease-like outer membrane protein autotransporters. Mol. Microbiol. **18**:378–380.
33. **Junker M, et al.** 2006. Pertactin beta-helix folding mechanism suggests common themes for the secretion and folding of autotransporter proteins. Proc. Natl. Acad. Sci. U. S. A. **103**:4918–4923.
34. **Kaper JB, Nataro JP, Mobley HL.** 2004. Pathogenic *Escherichia coli.* Nat. Rev. Microbiol. **2**:123–140.
35. **Kjaergaard K, Schembri MA, Ramos C, Molin S, Klemm P.** 2000. Antigen 43 facilitates formation of multispecies biofilms. Environ. Microbiol. **2**:695–702.
36. **Klemm P, Schembri MA.** 2000. Bacterial adhesins: function and structure. Int. J. Med. Microbiol. **290**:27–35.
37. **Korea CG, Badouraly R, Prevost MC, Ghigo JM, Beloin C.** 2010. *Escherichia coli* K-12 possesses multiple cryptic but functional chaperone-

Downloaded from http://iai.asm.org/ on December 23, 2011 by INSTITUT PASTEUR-Médiathèque

usher fimbriae with distinct surface specificities. Environ. Microbiol. **12**: 1957–1977.
38. **Kuehn MJ, Heuser J, Normark S, Hultgren SJ.** 1992. P pili in uropathogenic *E. coli* are composite fibres with distinct fibrillar adhesive tips. Nature **356**:252–255.
39. **Letunic I, Doerks T, Bork P.** 2009. SMART 6: recent updates and new developments. Nucleic Acids Res. **37**:D229–D232.
40. **Marchler-Bauer A, et al.** 2009. CDD: specific functional annotation with the conserved domain database. Nucleic Acids Res. **37**:D205–D210.
41. **Marchler-Bauer A, et al.** 2011. CDD: a conserved domain database for the functional annotation of proteins. Nucleic Acids Res. **39**:D225–D229.
42. **Melican K, et al.** 2011. Uropathogenic *Escherichia coli* P and type 1 fimbriae act in synergy in a living host to facilitate renal colonization leading to nephron obstruction. PLoS Pathog. **7**:e1001298.
43. **Miller JH.** 1992. A short course in bacterial genetics: a laboratory manual and handbook for *Escherichia coli* and related bacteria, vol. 1. Cold Spring Harbor Laboratory Press, Cold Spring Harbor, NY.
44. **Mobley HL, et al.** 1990. Pyelonephritogenic *Escherichia coli* and killing of cultured human renal proximal tubular epithelial cells: role of hemolysin in some strains. Infect. Immun. **58**:1281–1289.
45. **Muller CM, et al.** 2006. Role of histone-like proteins H-NS and StpA in expression of virulence determinants of uropathogenic *Escherichia coli.* J. Bacteriol. **188**:5428–5438.
46. **Mulvey MA, et al.** 1998. Induction and evasion of host defenses by type 1-piliated uropathogenic *Escherichia coli.* Science **282**:1494–1497.
47. **Mysorekar IU, Hultgren SJ.** 2006. Mechanisms of uropathogenic *Escherichia coli* persistence and eradication from the urinary tract. Proc. Natl. Acad. Sci. U. S. A. **103**:14170–14175.
48. **Ochman H, Selander RK.** 1984. Standard reference strains of *Escherichia coli* from natural populations. J. Bacteriol. **157**:690–693.
49. **Oelschlaeger TA, Dobrindt U, Hacker J.** 2002. Virulence factors of uropathogens. Curr. Opin. Urol. **12**:33–38.
50. **Parham NJ, et al.** 2004. PicU, a second serine protease autotransporter of uropathogenic *Escherichia coli.* FEMS Microbiol. Lett. **230**:73–83.
51. **Purdy GE, Fisher CR, Payne SM.** 2007. IcsA surface presentation in *Shigella flexneri* requires the periplasmic chaperones DegP, Skp, and SurA. J. Bacteriol. **189**:5566–5573.
52. **Reisner A, Haagensen JA, Schembri MA, Zechner EL, Molin S.** 2003. Development and maturation of *Escherichia coli* K-12 biofilms. Mol. Microbiol. **48**:933–946.
53. **Roberts JA, et al.** 1994. The Gal(α1–4)Gal-specific tip adhesin of *Escherichia coli* P-fimbriae is needed for pyelonephritis to occur in the normal urinary tract. Proc. Natl. Acad. Sci. U. S. A. **91**:11889–11893.
54. **Roos V, Schembri MA, Ulett GC, Klemm P.** 2006. Asymptomatic bacteriuria *Escherichia coli* strain 83972 carries mutations in the *foc* locus and is unable to express F1C fimbriae. Microbiology **152**:1799–1806.
55. **Roux A, Beloin C, Ghigo JM.** 2005. Combined inactivation and expression strategy to study gene function under physiological conditions: application to identification of new *Escherichia coli* adhesins. J. Bacteriol. **187**:1001–1013.
56. **Ruiz-Perez F, et al.** 2009. Roles of periplasmic chaperone proteins in the biogenesis of serine protease autotransporters of *Enterobacteriaceae.* J. Bacteriol. **191**:6571–6583.
57. **Ruiz-Perez F, Henderson IR, Nataro JP.** 2010. Interaction of FkpA, a peptidyl-prolyl cis/trans isomerase with EspP autotransporter protein. Gut Microbes **1**:339–344.
58. **Sambrook J, Russell DW.** 2001. Molecular cloning: a laboratory manual, 3rd ed. Cold Spring Harbor Laboratory Press, Cold Spring Harbor, NY.
59. **Sauri A, et al.** 2009. The Bam (Omp85) complex is involved in secretion of the autotransporter haemoglobin protease. Microbiology **155**: 3982–3991.
60. **Schembri MA, Blom J, Krogfelt KA, Klemm P.** 2005. Capsule and fimbria interaction in *Klebsiella pneumoniae.* Infect. Immun. **73**: 4626–4633.
61. **Schembri MA, Dalsgaard D, Klemm P.** 2004. Capsule shields the function of short bacterial adhesins. J. Bacteriol. **186**:1249–1257.
62. **Schembri MA, Kjaergaard K, Klemm P.** 2003. Global gene expression in *Escherichia coli* biofilms. Mol. Microbiol. **48**:253–267.
63. **Schembri MA, Klemm P.** 2001. Biofilm formation in a hydrodynamic environment by novel FimH variants and ramifications for virulence. Infect. Immun. **69**:1322–1328.
64. **Sherlock O, Schembri MA, Reisner A, Klemm P.** 2004. Novel roles for the AIDA adhesin from diarrheagenic *Escherichia coli*: cell aggregation and biofilm formation. J. Bacteriol. **186**:8058–8065.
65. **Simon R, Priefer U, Puhler A.** 1983. A broad host range mobilization system for *in vivo* genetic engineering: transposon mutagenesis in Gram-negative bacteria. Nat. Biotechnol. **1**:784–791.
66. **Stamm WE, Norrby SR.** 2001. Urinary tract infections: disease panorama and challenges. J. Infect. Dis. **183** Suppl. 1:S1–4.
67. **Svanborg-Eden C, et al.** 1987. Bacterial virulence versus host resistance in the urinary tracts of mice. Infect. Immun. **55**:1224–1232.
68. **Ulett GC, Mabbett AN, Fung KC, Webb RI, Schembri MA.** 2007. The role of F9 fimbriae of uropathogenic *Escherichia coli* in biofilm formation. Microbiology **153**:2321–2331.
69. **Ulett GC, et al.** 2007. Functional analysis of antigen 43 in uropathogenic *Escherichia coli* reveals a role in long-term persistence in the urinary tract. Infect. Immun. **75**:3233–3244.
70. **Ulett GC, Webb RI, Schembri MA.** 2006. Antigen-43-mediated autoaggregation impairs motility in *Escherichia coli.* Microbiology **152**: 2101–2110.
71. **Ussery DW, Higgins CF, Bolshoy A.** 1999. Environmental influences on DNA curvature. J. Biomol. Struct. Dyn. **16**:811–823.
72. **Valle J, et al.** 2008. UpaG, a new member of the trimeric autotransporter family of adhesins in uropathogenic *Escherichia coli.* J. Bacteriol. **190**: 4147–4161.
73. **Vlahovicek K, Kajan L, Pongor S.** 2003. DNA analysis servers: plot.it, bend.it, model.it and IS. Nucleic Acids Res. **31**:3686–3687.
74. **Wagner JK, Heindl JE, Gray AN, Jain S, Goldberg MB.** 2009. Contribution of the periplasmic chaperone Skp to efficient presentation of the autotransporter IcsA on the surface of *Shigella flexneri.* J. Bacteriol. **191**: 815–821.
75. **Wells TJ, et al.** 2009. The *Escherichia coli* O157:H7 EhaB autotransporter protein binds to laminin and collagen I and induces a serum IgA response in O157:H7 challenged cattle. Environ. Microbiol. **11**:1801–1814.
76. **Wells TJ, et al.** 2008. EhaA is a novel autotransporter protein of enterohemorrhagic *Escherichia coli* O157:H7 that contributes to adhesion and biofilm formation. Environ. Microbiol. **10**:589–604.
77. **Wells TJ, Totsika M, Schembri MA.** 2010. Autotransporters of *Escherichia coli*: a sequence based characterisation. Microbiology **156**: 2459–2469.
78. **Wiles TJ, Kulesus RR, Mulvey MA.** 2008. Origins and virulence mechanisms of uropathogenic *Escherichia coli.* Exp. Mol. Pathol. **85**:11–19.
79. **Wu XR, Sun TT, Medina JJ.** 1996. *In vitro* binding of type 1-fimbriated *Escherichia coli* to uroplakins Ia and Ib: relation to urinary tract infections. Proc. Natl. Acad. Sci. U. S. A. **93**:9630–9635.
80. **Wullt B, et al.** 2000. P fimbriae enhance the early establishment of *Escherichia coli* in the human urinary tract. Mol. Microbiol. **38**:456–464.
81. **Yamada H, Muramatsu S, Mizuno T.** 1990. An *Escherichia coli* protein that preferentially binds to sharply curved DNA. J. Biochem. **108**: 420–425.
82. **Zdobnov EM, Apweiler R.** 2001. InterProScan-an integration platform for the signature-recognition methods in InterPro. Bioinformatics **17**: 847–848.
83. **Zhang Y.** 2008. I-TASSER server for protein 3D structure prediction. BMC Bioinformatics **9**:40.

Downloaded from http://iai.asm.org/ on December 23, 2011 by INSTITUT PASTEUR-Médiathèque